Progress In Electromagnetics Research C, Vol. 29, 41–53, 2012

PASSIVE COMPENSATION OF BEAM SHIFT IN A BENDING ARRAY

T. J. Seidel[1, 2, *], W. S. T. Rowe[1, 2], and K. Ghorbani[1, 2]

[1]School of Electrical and Computer Engineering, RMIT University, Melbourne 3001, Australia

[2]Defence Materials Technology Centre (DMTC), Australia

Abstract—An array of conformal antenna structures mounted on a bending surface exhibits a substantial shift in main beam direction. This paper demonstrates a method to compensate for the induced beam shift by using the change in length of the surface produced by the bend. This change in length modifies the capacitance in a composite right/left-handed transmission (CRLHTL) line, causing a phase shift in the line. A potential implementation is proposed that can correct an 18° beam shift with only an induced change in length of 0.144%. The paper establishes that this passive compensation concept is feasible and provides significant benefits over active compensation systems in terms of weight reduction, cost, simplification and the ability to operate in radio silence.

1. INTRODUCTION

Conformal Load-bearing Antenna Structures (CLAS) provide significant advantages in weight reduction and antenna robustness over traditional antennas attached to the exterior of airborne platforms. Seminal papers by Lockyer et al. [1, 2] and Callus [3] suggest increased focus on applying CLAS to civilian and military aircraft. Much of the research into CLAS is centered on structural integrity to ensure that any CLAS fitted to an aircraft will meet the stringent structural requirements required during flight. The bending a CLAS is subjected to when fitted to a highly flexible component such as an airplane wing poses substantial challenges to the preservation of antenna performance. The movement of a flexible mounting platform under an antenna array results in distortion and redirection of the radiation patterns.

Received 4 March 2012, Accepted 12 April 2012, Scheduled 23 April 2012

* Corresponding author: Toby Joel Seidel (toby.seidel@rmit.edu.au).

The effect of wing bending on radiation patterns emanating from an antenna array has been previously modeled [4, 5]. In [4], it was demonstrated that beam direction was significantly impacted under standard aircraft operation. Furthermore, an active control system was proposed to sense wing deformation and correct for the resultant shift in beam direction. A strain based approach was introduced in [6] to instantaneously determine beam direction shifts and actively compensate for them. Another approach for self calibration of beam direction was proposed in [7], which is reliant on multiple sensors to predict deformation using a two step Constant Modulus approach.

Whilst these and other active calibration methods have been demonstrated to address radiation pattern distortion exhibited under bending conditions, they require extra processing power and add weight to an aircraft. In addition, they rely on robust sensors which therefore add to maintenance requirements. These sensors also may require additional wiring systems to be added to the aircraft loom and further compound weight restrictions. Ideally, a passive compensation system would be preferable.

This paper examines the feasibility of a novel passive main beam compensation technique. This technique utilizes the physical deformation of an aircraft wing to induce changes in composite right/left-handed transmission lines [8] (CRLHTL) implemented with tunable inter-digital capacitors. The deformation as the wing bends leads to a small change in length (strain) which will be used to tune the inter-digital capacitors.

The CRLHTL was selected as they have been shown to exhibit higher tunability than right-handed transmission lines [9–11]. The effect of the bending surface on the performance of the compensation technique is also considered, to determine the nature and magnitude of phase shift required. This paper considers antenna arrays operating with a center frequency of 10 GHz.

2. BEHAVIOR OF A BENDING ARRAY

To model the effects of a bending surface on an antenna array a 10 element linear array operating at 10 GHz was simulated using CST Microwave Studio. Each element of the array was spaced at a half wavelength and the array was considered to be mounted on a 2 m semi rigid surface with the first element starting at the center point of the surface. One end of the surface is fixed allowing one degree of freedom for bending at the other end (Fig. 1). Each element of the array is fed with an individual microstrip line mounted on a malleable undercarriage to allow for phase variation between elements. The array

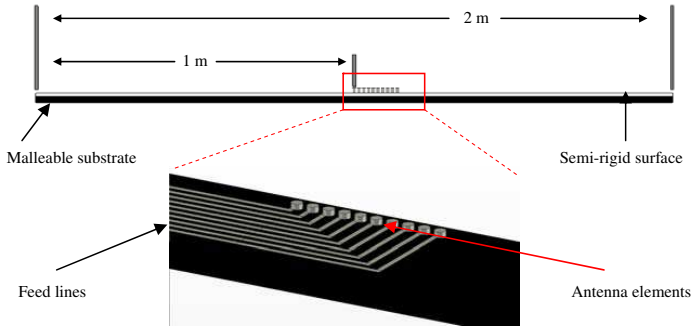

Figure 1. Simple representation of the modeled surface showing representative feed lines and antenna elements (zoomed area).

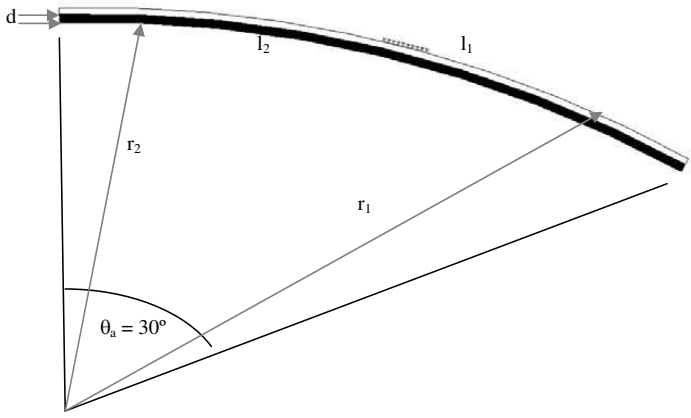

Figure 2. Modeled surface under a 30° clockwise bend.

was simulated assuming the surface was flat and the bent with an arc of 30° (Fig. 2).

The simulated radiation patterns for the array are shown in Figs. 3 and 4 for the flat surface and a 30° clockwise arc or bend (Fig. 2) respectively. A significant change in beam direction −18° is observed between Fig. 3 and Fig. 4. However the beamwidth, side lobe levels and gain change by less than 2%. This is due to the very small physical angle between each antenna element. In the above described case the change in angle between each element is just 0.675°, and therefore just over 6° from the first element to the last. This leads to minimal change in the physical properties of the radiation pattern. As a result the radiation pattern can be approximated to that of a flat array normal

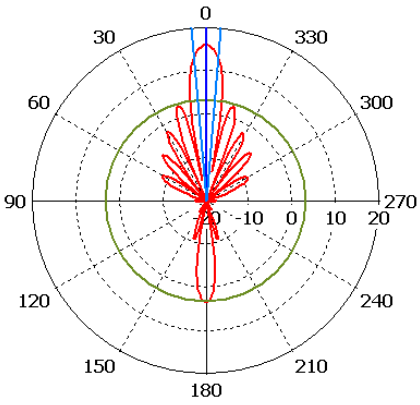

Figure 3. Radiation pattern of the array on a flat surface — main beam angle 0°, beamwidth 10°.

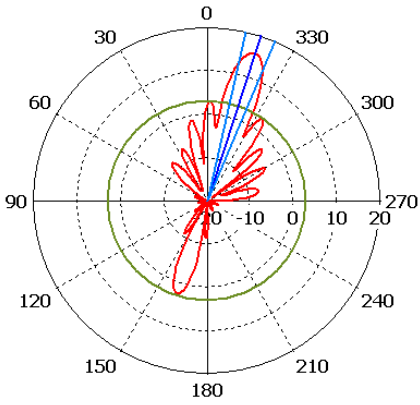

Figure 4. Radiation pattern of the array on a surface with a 30° bend — main beam angle shifted by 18°, beamwidth 10.1°.

to the center of the array. Therefore a bend of 30° results in a main beam shift of 18°. Using conventional array theory, a phase shift of 55.6° between each array element can be used to correct beam angle back to that of the unbent array. The inverse is true for anti-clockwise bends as the change in angle between each element is still very small and therefore a negative bend of 30° would correspond to a +18° shift in beam direction.

Figure 5 shows that when a simple progressive phase shift is applied between each element of an array on a surface with a 30° bend, the radiation pattern is once again directed towards 0°. This redirection has led to a slight increase in main beam width of 0.5°. The gain and side lobe levels are largely unaffected with a less than 3% change after beam correction.

3. PASSIVE COMPENSATION

The method of passive compensation proposed in this paper uses a CRLHTL configured in a T-network structure with series equivalent capacitors and a parallel inductance. The proposed design consists of microstrip Inter-Digital Capacitor (IDC) components and a shunt inductor as seen in Fig. 6. The structure creates a phase shift by using the strain (or change in length) in a surface to vary the separation between each side of the inter-digital capacitors. To achieve this each side of the IDC must be physically disconnected from each other. Also

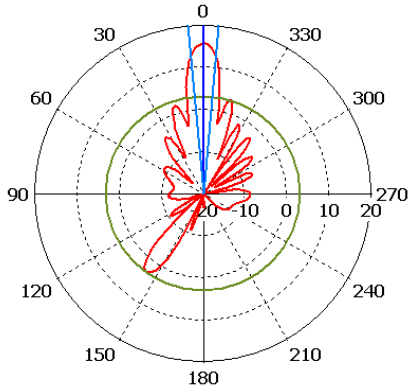

Figure 5. Radiation pattern of the array on a surface with a 30° bend, and a 55.6° progressive phase shift between elements. Main beam angle 0°, beamwidth 10.5°.

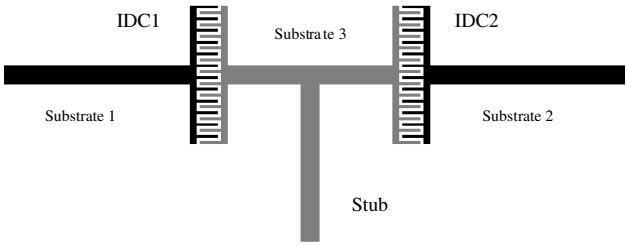

Figure 6. Single segment CRLHTL consisting of IDCs with 12 fingers and a shunt inductor.

the center section of the structure must be fixed to the bending surface allowing the outer sides to move towards or away from the center.

The approximate equivalent circuit for the T-network structure (Fig. 6) is shown in Fig. 7. Each IDC has a capacitance related to the gap between each side (C_g). L_f is the inductance of the very thin interdigital fingers and L_s is the inductance generated by the microstrip stub. Each unconnected section of microstrip line has an inherent capacitance to ground (C_{ms}) and there is some amount of loss leading to an equivalent resistance (R_{ms}). The effect of the transmission lines in the structure also need to be considered as they will have significant effect on the phase response. In the above example a half wavelength transmission line is inserted in-between the IDC and stub to clearly show each element. Ideally the IDC and stub could be

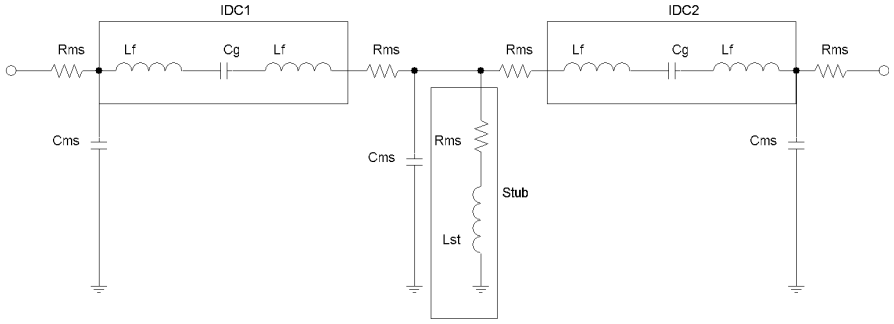

Figure 7. Equivalent circuit of Fig. 5.

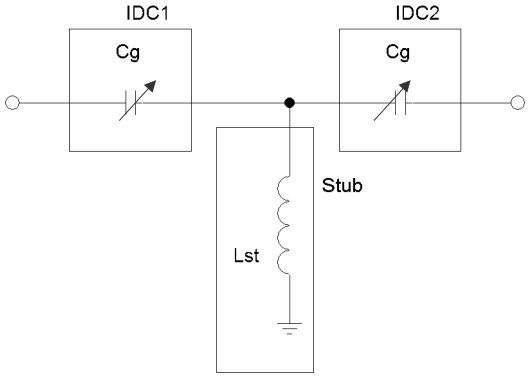

Figure 8. Simplified equivalent circuit.

directly connected as is traditional in CRLHTL structures [8]. The full design of the structure needs to take into account each of the above mentioned elements, however, only C_g changes when the IDC separation changes [8, 12]. The circuit can then be simplified into the interdigital gap capacitance (C_g) and the stub inductor (L_s) (Fig. 8) which is used to make initial designs with desirable phase shifts. The design can then be refined to account for the other elements using simulation software such as ADS and CST as was done in this case.

The phase constant of a single CRLHTL T-network structure can be described as:

$$\beta = -\frac{\sqrt{2}}{\omega\sqrt{LC}} \tag{1}$$

where L is the total inductance and C is the inter-digital capacitance. Since the only change in the model generated by modifying the gap

between the IDCs is the interdigital capacitance (C_g), the phase shift generated by a change in capacitance in the structure in Fig. 4 will be:

$$\Delta\varphi = -\frac{\sqrt{2}}{\omega\sqrt{L}}\left(\frac{1}{\sqrt{C_2}} - \frac{1}{\sqrt{C_1}}\right) \tag{2}$$

where C_1 is the initial total capacitance of the T-network and C_2 is the final total capacitance.

A change in length is induced in the malleable substrate by bending the semi-rigid surface. Since the bend angle is the same but the equivalent radius of the arc is different there must be a change in the arc length. This change is directly proportional to the malleable substrate thickness (Eq. (3))

$$l_2 = \frac{l_1 r_1}{r_2} \tag{3}$$

where l_1 is the length of the semi-rigid surface, l_2 is the length of the malleable substrate, r_1 is the radius of the semi-rigid surface's arc and r_2 is the radius of the malleable substrate's arc given in Eqs. (4) and (5).

$$r_1 = l_1 \frac{360}{2\pi\theta_a} \tag{4}$$

$$\begin{aligned} r_2 &= r_1 - d \qquad \theta_a > 0 \\ r_2 &= r_1 + d \qquad \theta_a < 0 \end{aligned} \tag{5}$$

where θ_a is the bend angle and d is the thickness of the semi-rigid surface and the malleable substrate. The malleable substrate increases in length in the case of a negative bend.

In this case, a 5 mm thick malleable substrate would give an overall change in length of 2.6 mm if the semi-rigid surface was bent to 30°.

The proposed passive compensation system makes use of a large number of tunable CRLHTL structures spaced along the length of a long bending surface.

3.1. Prototype Device

To achieve the required phase response a 12 fingered IDC CRLHTL device was designed on Rogers RT/duroid 5880 substrate ($\varepsilon_r = 2.2$, $\tan\delta = 0.0009$, thickness = 0.508 mm with 0.5 oz copper). Each IDC finger has a width and spacing (gap) of 0.2 mm. The initial separation between the ends of the interdigital fingers and the sides of the IDC element is 0.12 mm. Microstrip feed lines are 1.5 mm wide and the inductive stub is 10.7 mm long.

The device needs to be constructed from three independent substrates (Fig. 6) to allow the IDCs to separate properly while keeping the microstrip tracks in the same plane. A CST model of the structure is presented in Fig. 9. Since the feature size of the IDC is very small, cutting the substrate between each finger to allow separation is not feasible. To ensure the physical disconnect between the capacitors the two outer arms (dark lines in Fig. 9) were placed on two grounded substrates that are separated by a single split down the middle. A third ungrounded substrate contains the inner arms of the capacitor and the shunt inductor (light lines in Fig. 9). The third substrate sits on top of the two grounded substrates with the microstrip line facing down.

As the effect of the bent array surface is simply a change in length and the bend across each element is very small, the structure was simulated and measured by only changing the separation between the end of the fingers and the sides of the IDC elements. The structure of Fig. 8 was simulated in CST with IDC separations of 0, ± 10, ± 20, ± 25, ± 30, ± 40 and $\pm 50\,\mu$m. The phase results are displayed in Table 1.

A single segment of the IDC CRLHTL device was produced using the same parameters as the simulated device of Fig. 9, and mounted onto a moving stage controlled by a micrometer (Fig. 10). The micrometer platform allowed for an accurate resolution step of no less than $25\,\mu$m, hence measurements could only be reliable taken at the

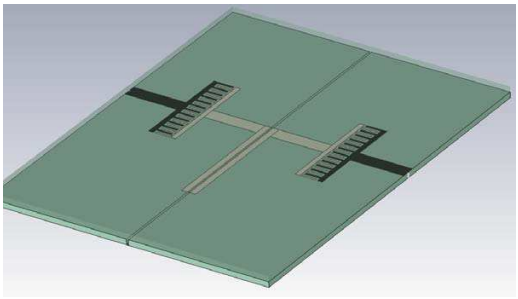

Figure 9. The CST simulation schematic of the prototype three substrate IDC CRLHTL structure. The dark microstrip lines are on the lower substrates, whilst the light microstrip line is on the underside of a transparent top substrate. All microstrip lines are in the same plane.

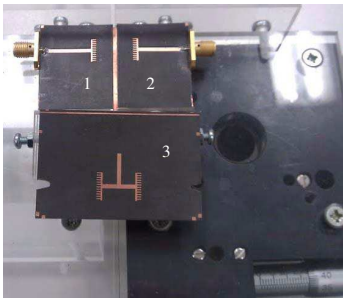

Figure 10. The prototype of the three substrate IDC CRLHTL structure on moving stage with the three substrates identified (substrate 3 has been flipped over to expose the metallic pattern).

Table 1. Relative phase shift for the three substrate IDC CRLHTL structure.

Bend angle (θ)	**Extension (μm)**	**Simulated $\Delta\varphi$ (degrees)**	**Measured $\Delta\varphi$ (degrees)**
30 clockwise	−50	−17.0	−17.3
24 clockwise	−40	−14.0	
21 clockwise	−30	−9.9	
18 clockwise	−25	−8.5	−8.9
12 clockwise	−20	−6.5	
6 clockwise	−10	−2.3	
0 (reference)	0	0	0
6 anti-c'wise	10	4.1	
12 anti-c'wise	20	7.9	
18 anti-c'wise	25	9.3	8.6
21 anti-c'wise	30	11.5	
24 anti-c'wise	40	14.2	
30 anti-c'wise	50	16.9	17

0, ±25 and ±50 μm positions. Measurements of the phase of S_{21} were performed using a Wiltron Vector Network Analyser (VNA) and these results are also displayed in Table 1. The measured phase changes are within 10% of the simulated results. As the device requires the alignment of three hidden microstrip line structures to within 50 μm of each other, it is possible that the error is the result of a slight misalignment.

3.2. Required Number of Elements

The array example in Section 2 requires a phase shift of 55.6° per antenna element to compensate for a 30° bend. A relative phase shift of around 17° was measured for the prototype three substrate IDC CRLHTL structure. Hence at least four of these devices would be needed to obtain the required phase shift, however, this would result in a total shift of 68°. Therefore these four IDC CRLHTL devices would need to be tuned to obtain the desired phase shift for each bending angle. This could be achieved by using three of the above described CRLHTL devices and an additional IDC CRLHTL device with a smaller phase shift per extension, implemented with fewer IDC fingers.

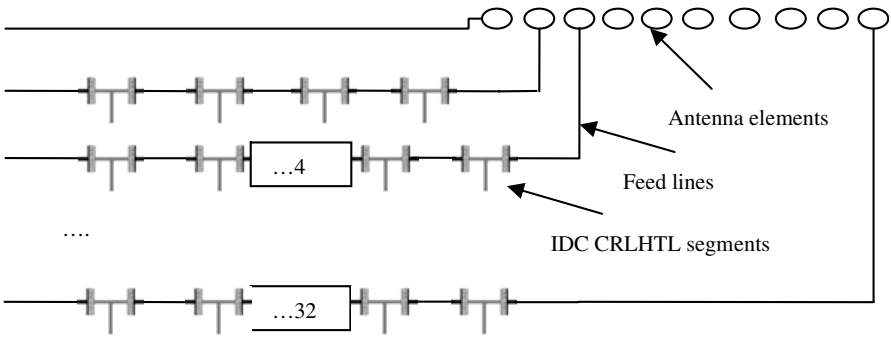

Figure 11. Representation of a proposed antenna feed network. First antenna has no moving IDC elements. Each subsequent antenna as an additional 4 moving IDC elements.

An alternative method would be to change the height of the malleable substrate that the CRLHTL structure is mounted on. By setting it to 5.5 mm from the bending surface the extension will be reduced to 40 μm per element over the 30° bend. This would lead to a maximum required extension over the whole feeding structure of 1.44 mm or 0.144% of the feed length. Overall the total number of segments per feeding line would be 36 giving a total length of around 0.9 m, making it ideal for the proposed application. This would correct the resulting shift from all bend angles providing the system is sufficiently linear. The resultant feed network is shown in block form in Fig. 11.

3.3. Non-linearity

Since the induced change in length, beam shift, and progressive phase required to correct the beam shift of a bent array all exhibit a linear response to the bending angle, it is important that the behavior of each IDC CRLHTL structure is also linear. From Table 1, the average phase change per micro meter is 0.34°. This shows that the largest deviation for a clockwise bend occurs at −10 μm (or an equivalent bend angle of 6°) and for a anti-clockwise bend at 30 μm (bend angle of 21°).

The effect of the non-linearity can be examined by applying the resultant phase shifts to the bending array simulation. To provide the largest range of results it will be assumed that there are 4 CRLHTL structures progressive per array element. This will produce a 56° phase shift at 40 μm.

Table 2 shows that in all the negative bending cases the resultant main beam direction is almost completely corrected, with an error of

Table 2. Effect of non-linearity on beam correction.

Bend (°)	**Simulated Δ in beam direction** (°)	**Required Δφ** (°)	**Simulated Δφ** (°)	**Corrected beam Direction** (°)
−30	−18	−55.6	−56	0
−24	−14.4	−44.5	−42.3	$< \|1\|$
−18	−10.8	−33.3	−31.4	$< \|1\|$
−12	−7.2	−22.2	−18.9	$< \|1\|$
−6	−3.6	−11.2	−9.3	$< \|1\|$
6	3.6	11.2	13.6	$< \|1\|$
12	7.2	22.2	24.6	−1
18	10.8	33.3	37	−1
24	14.4	44.5	48.1	−1
30	18	55.6	56.8	$< \|1\|$

less than 1°. The results for a positive bend are also good, with slight correction errors in the vicinity of 1°. These positive bend results are due to the tendency for the phase shift in the positive direction to be marginally higher than for negative bends. This could be alleviated by increasing the initial separation to balance the linearity for positive and negative bends. Overall, the effect of the non-linearity in this structure is very small and is unlikely to adversely affect the performance of this technique.

4. CONCLUSION

This paper demonstrates the feasibility of a device for passively compensating the redirected main beam from an array on a bending surface. The device uses a CRLHTL structure formed using a T-network of series IDCs and a shunt inductor. The device can correct the directionality of an array placed on a substantially bending surface with only a small extension or compression through the CRLHTL feeding network. An 18° change in directionality was corrected with only a 0.144% change in length of the overall structure. The device can provide significant advantages over active systems in terms of weight, cost and energy consumption. As the system is entirely passive, it will continue to operate in situations where radio silence is necessary.

ACKNOWLEDGMENT

This research was partly conducted within the Defence Materials Technology Centre, which was established and is supported by the Australian Government's Defence Future Capability Technology Centre (DFCTC) initiative.

REFERENCES

1. Lockyer, A. J., J. N. Kudva, D. M. Kane, B. P. Hill, C. A. Martin, A. C. Goetz, and J. Tuss, "A qualitative assessment of smart skins and avionic/structures integration," *SPIE Conference on Smart Structures and Materials*, Vol. 2189, 172–183, Orlando, Florida, USA, Feb. 14, 1994.
2. Lockyer, A. J., K. H. Alt, D. P. Coughlin, M. D. Durham, J. N. Kudva, A. C. Goetz, and J. Tuss, "Design and development of a conformal load-bearing smart-skin antenna: Overview of the AFRL smart skin structures technology demonstration (S3TD) program," *SPIE Conference on Smart Structures and Materials*, Vol. 3674, 410–424, Newport Beach, California, USA, Mar. 1999.
3. Callus, P. J., "Conformal load bearing antenna structure for Australian defence force aircraft," DSTO Technical Report, 40, DSTO-TR-1963, Mar. 2007, http://hdl.handle.net/1947/8164.
4. Smallwood, B. P., R. A. Canfield, and A. J. Terzuoli, Jr., *Structurally Integrated Antennas on a Joined-wing Aircraft*, Collection of Technical Papers — AIAA/ASME/ASCE/AHS/ASC Structures, Structural Dynamics and Materials Conference, Vol. 1, 549–556, 2003.
5. Seidel, T. J., W. S. T. Rowe, and K. Ghorbani, "Passive compensation of beam shift in an array on a bending surface," *2011 European Radar Conference (EuRAD)*, 85–88, Manchester, UK, Oct. 12–14, 2011.
6. Banks, D., M. Berden, B. Baron, and J. Tenbarge, "Structurally integrated X-band array development," *Multifunctional Structures/Integration of Sensors and Antennas*, 17-1–17-12, 2006.
7. Santori, A., J. Barrère, G. Chabriel, C. Jauffret, and D. Medynski, "Array shape self-calibration for large flexible antenna," *IEEE Aerospace Conference Proceedings*, No. 4161477, 2007.
8. Caloz, C. and T. Itoh, *Electromagnetic Metamaterials: Transmission Line Theory and Microwave Applications, the Engineering Approach*, John Wiley & Sons, New York, 2006, ISBN-10: 0-471-66985-7.

9. Damm, C., M. Schussler, M. Oertel, and R. Jakoby, "Compact tunable periodically LC loaded microstrip line for phase shifting applications," *IEEE MTT-S International Microwave Symposium*, Vol. 1–4, 2003–2006, Long Beach, CA, Jun. 2005.
10. Sheng, S., P. Wang, and C. K. Ong, "Compact tunable periodically LC loaded phase shifter using left-handed transmission line," *Microwave and Optical Technology Letters*, Vol. 51, No. 9, 2127–2129, 2009.
11. Hongjoon, K., S.-J. Ho, M.-K. Choi, A. B. Kozyrev, and D. W. van der Weide, "Combined left- and right-handed tunable transmission lines with tunable passband and 0 phase shift," *IEEE Transactions on Microwave Theory and Techniques*, Vol. 54, No. 12, 4178–4184, Dec. 2006.
12. Bahl, I., *Lumped Elements for RF and Microwave Circuits*, Artech House Microwave Library, Norwood, MA, 2003, ISBN 1-58053-309-4.